# CHAPTER VI

## MAGNETIC AND ELECTRIC BIREFRINGENCE IN THE ISOTROPIC PHASE OF NEMATIC LIQUID CRYSTALS

The first magnetic birefringence measurements in the isotropic phase of nematics were performed by Zadoc-Kahn[1] on PAA. She showed that in the neighbourhood of $T_{NI}$ the magnetic birefringence can be as much as 100 times greater than in ordinary organic liquids like nitrobenzene. This is a direct evidence of the persistence of the nematic-like short range order fa the isotropic phase even after the vanishing of the long range order at $T_{NI}$. Foex[2] in 1933 observed that the magnetic birefringence in the isotropic phase exhibits a $(T - T^{*})^{-1}$ dependence and this behaviour is closely analogous to that of a ferromagnet above the Curie temperature. Similar anomalies are observed in the electric birefringence also. These short range order effects in the isotropic phase can be described

in terms of a phenomenological model proposed by de Gennes,[3] based on the Landau theory[4] of phase transitions.

Landau-de Gennes model

Consider an expansion of the excess free energy of any ordered system in powers of a scalar order parameter s in the following form:

$$F = \frac{1}{2}As^2 - \frac{1}{3}Bs^3 + \frac{1}{4}Cs^4 + \ldots \qquad (6.1)$$

The term of order $s^3$ is not precluded by symmetry since s and -s represent two entirely different physical arrangements of the molecules. When $B > 0$, (6.1) leads to a first order phase transition. But when $B = 0$ the transition is of second order and A may be taken as

$$A = a(T - T^*) ,$$

where $T^*$ is the transition temperature. Even when the nematic-isotropic transition is first order, we may

retain the same form of A(T) with $T^*$ now representing a hypothetical second order transition point slightly below $T_{NI}$. The form of A(T) is determined[4] by the fact that A vanishes at the transition point, being positive on one side of the transition and negative on the other. In the disordered phase $s = 0$ corresponds to a minimum of F only if $A > 0$, while in the ordered phase $s \neq 0$ corresponds to a minimum only if $A < 0$.

Bath F and $\partial F/\partial s$ vanish at the transition point $T_{NI}$. Neglecting the higher order terms, the first condition can be written as

$$F = \tfrac{1}{2}As^2 - \tfrac{1}{3}Bs^3 + \tfrac{1}{4}Cs^4 = 0 .$$

Elimination of $s^2$ leads us to a quadratic equation in s the solutions of which are given by

$$s = \frac{\tfrac{1}{3}B \pm \sqrt{\tfrac{1}{9}B^2 - \tfrac{1}{2}AC}}{\tfrac{1}{2}C} . \qquad (6.2)$$

The roots of s are real only if

$$A \leqslant \frac{2B^2}{9C}$$

from which we get, at the transition,

$$T_{NI} - T^* = \frac{2B^2}{9aC}$$

and

$$s_o = \frac{2B}{3C} \cdot \qquad (6.3)$$

The value of B is small since the nematic-isotropic transition is weakly first order and therefore $(T_{NI} - T^*)$ may be expected to be a very small quantity.

## i. Magnetic birefringence

In the presence of an external magnetic field H, there is an additional term in the free energy expression (6.1). This term is the average orientational potential energy due to the external field.

$$F = \frac{1}{2}a(T - T^*)s^2 - \frac{1}{3}B_A \Delta\chi \quad H^2 s \ , \qquad (6.4)$$

where $N_A$ is the Avogadro number and $\Delta\chi$ is the anisotropy of diamagnetic susceptibility for perfectly parallel alignment ($s = 1$). Here W have neglected the higher powers of $s$ since the magnetically induced order ($s_H$) is extremely weak ($\sim 10^{-5}$). The condition $\partial F/\partial s = 0$ leads to the result

$$s_H = \tfrac{1}{3}N_A \Delta\chi H^2/a(T - T^*) \quad . \qquad (6.5)$$

Thus the magnetic birefringence which is proportional to $s_H$ is given by

$$\Delta n_M = \frac{C_M}{a(T - T^*)} \quad .$$

$C_M$ can be determined[5] by assuming a Lorenz-Lorentz type of relationship for the refractive index n. Then

$$\Delta n_M = \frac{2\pi N_A^2 \Delta\chi \ \Delta\eta \ H^2(n^2 + 2)^2}{27Vn \ a(T - T^*)} \quad , \qquad (6.6)$$

where $\Delta\eta$ is the anisotropy of optical polarizability of the molecule and V the molar volume. Thus $\Delta n_M$

varies as $(T - T^*)^{-1}$ which is in accord with experiment.[2,6] Substituting $\Delta\eta = 25.9 \times 10^{-24}$ cm$^3$,[7] $\Delta\chi = 104.2 \times 10^{-a}\, a^3$[8] and H = 33,900 Gauss[1] for PAA, the experimental data of Zadoc-Kahn[1] for $\Delta n_M$ yield a = 27.4 J mole$^{-1}$ K$^{-1}$ and $T_{NI} - T^* = 1$ K[9] (see figure 6.1).

ii. Electric Birefringence

When Tsvetkov and Ryumtsev[10] measured the electric birefringence of PAA a most striking result was observed. The Kerr constant of PAA showed a reversal of sign at about $(T_{NI} + 5)$K (see figure 6.1). It was shown by Madhusudana and Chandrasekhar[9] that this is consistent with the phenomenological model when proper allowance is made for the contributions of the polarizability and permanent dipole moment to the free energy.

In the presence of an electric field E the orientational energy has contributions from (a) the

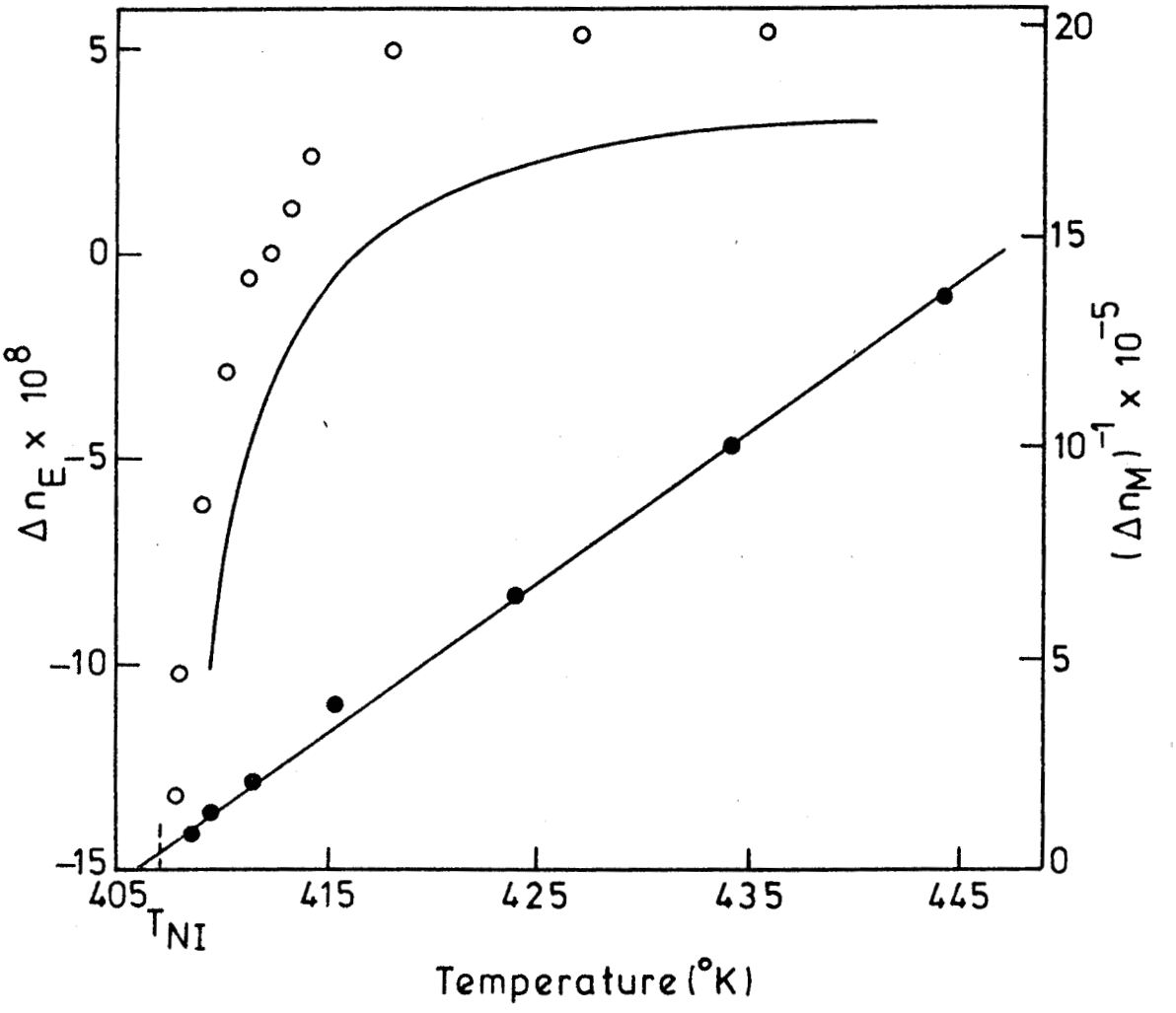


**Figure 6.1**

The electric birefringence (○) (after Tsvetkov and Ryumtsev[10]) and tho reciprocal of the magnetic birefringence (●) (after Zadoc-Kahn[1]) in the isotropic phase of PAA versus temperature. The lines represent the theoretical variations as calculated by Madhusudana and Chandrasekhar[9].

anisotropy of low frequency polarizability $\Delta\alpha$ and (b) the net permanent dipole moment $\mu$. The average orientational energy of the molecule due to the induced dipole moment is

$$W_1 = \frac{-\Delta\alpha}{5} F^2 h^2 E^2 s$$

and that due to the permanent dipole moment is

$$W_2 = -\frac{F^2 h^2 \mu^2 E^2}{6kT} (3\cos^2\beta - 1)s \quad .$$

All the symbols have already been explained in chapter II.

The free energy expansion takes the form

$$F = \frac{1}{2}a(T - T^*)s^2 - \frac{1}{5}N_A F^2 h^2 E^2 [\Delta\alpha - (F\mu^2/2kT)(1 - 3\cos^2\beta)]s \qquad (6.7)$$

from which we get the induced order parameter $s_E$ as

$$s_E = \frac{N_A F^2 h^2 E^2 [\Delta\alpha - (F\mu^2/2kT)(1 - 3\cos^2\beta)]}{9a(T - T^*)} \quad . \qquad (6.8)$$

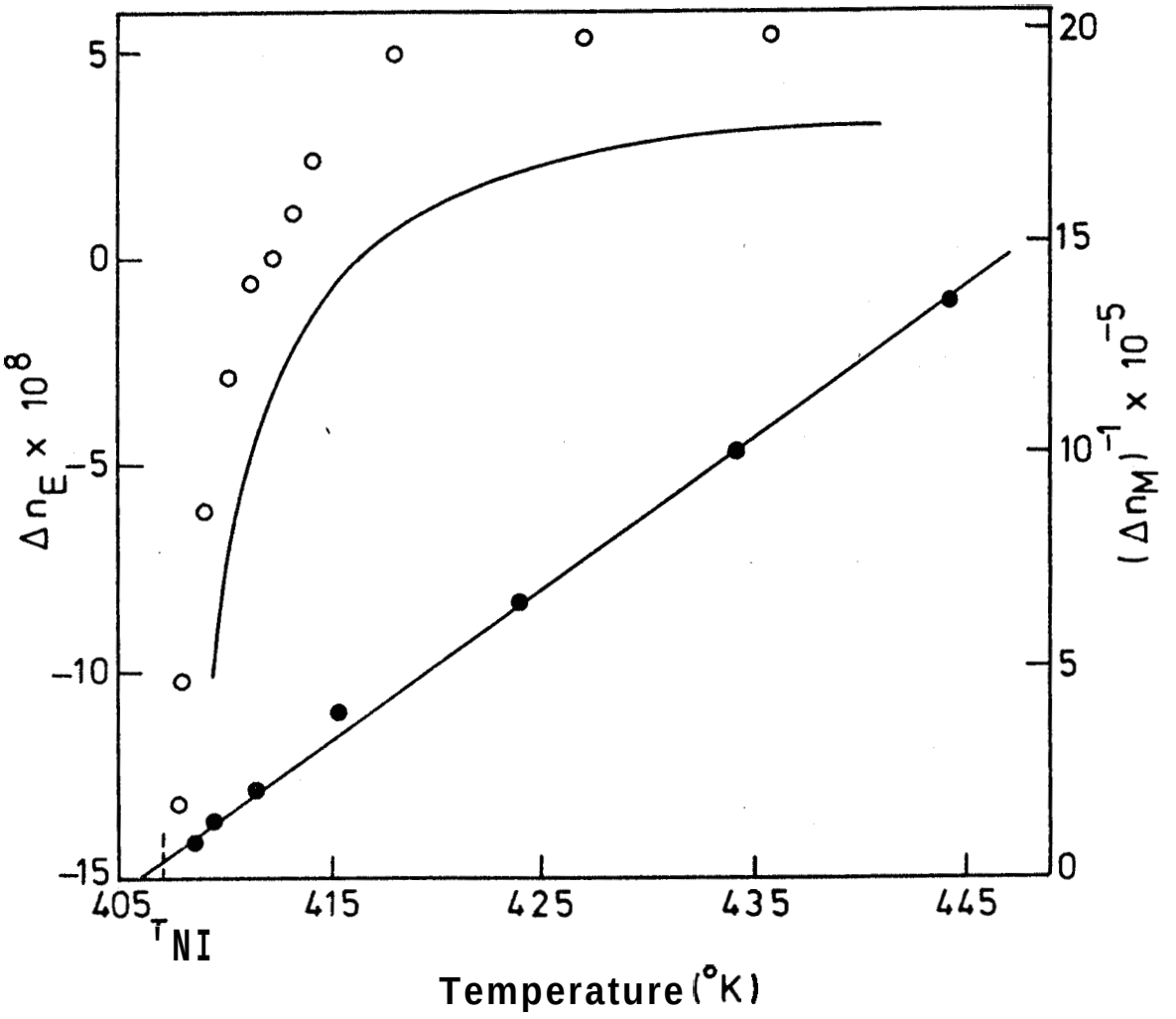


**Figure 6.1**

The electric birefringence (○) (after Tsvetkov and Ryumtsev[10]) and the reciprocal of the magnetic birefringence (●) (after Zadoc-Kahn[9]) in the isotropic phase of PAA versus temperature. The lines represent the theoretical variations as calculated by Madhusudana and Chandrasekhar[9].

The electric birefringence which is proportional to $s_E$ is given by

$$\Delta n_E = \frac{2\pi N_A^2 \Delta\eta (n^2+2)^2 F h^2 E^2 [\Delta\alpha - (F\mu^2/2kT)(1-3\cos^2\beta)]}{27nV_A(T - T^*)} \quad (6.9)$$

The values of $\mu$ and $\beta$ for PAA are estimated to be 2.2 debyes and 62.5° respectively from Kerr constant measurements in dilute solutions and dielectric measurements in the isotropic phase. Taking $\varepsilon = 5.65$ at $T_{NI} + 5K$,[11] $\Delta\alpha = 23 \times 10^{-24}$ cm$^3$, $E = 12$kV/cm along with the values of 'a' and $T_{NI} - T^*$ derived from the magnetic birefringence measurements, Madhusudana and Chandrasekhar calculated the variation of $\Delta n_E$ with temperature (see figure 6.1). Even though the theoretical curve very well demonstrates the reversal of sign of $\Delta n_E$, the temperature at which it occurs is higher ($T_{NI} + 9K$). This discrepancy is mainly due to the sensitiveness of the equation to the value of $\beta$.

Since there is a competition between the polarizability and the permanent dipole moment contributions even a mall error in $\beta$ will cause an appreciable shift in the temperature at which $\Delta n_E$ is zero.

According to (6.9), for small values of $\beta$ the value of $\Delta n_E$ is positive at all temperatures. Then the temperature variation of $\Delta n_E$ must be essentially similar to that of $\Delta n_M$. Small values of $\beta$ are realised in molecules having a large parallel component of the dipole moment. When the nematic liquid crystal is composed of such strongly polar molecules, energy considerations demand that the neighbouring molecules assume an antiparallel orientation. Madhusudana and Chandrasekhar[12] have applied their theory of antiparallel short range order to the isotropic phase of a nematic in which a weak long range order ($\sim 10^{-4}$ or less) baa been induced by an external (electric or magnetic) field. This model predicts that

both $\Delta n_M$ and $\Delta n_E$ should vary as $(T - T^*)^{-1}$. We studied two strongly positive nematic liquid crystals and showed experimentally for the first time that both $\Delta n_M$ and $\Delta n_E$ exhibit a $(T - T^*)^{-1}$ dependence with the same value of $T^*$, confirming the theoretical predictions.

## Experimental

### a. Sample

We undertook the measurement of $\Delta n_M$ and $\Delta n_E$ of two strongly positive compounds, viz., 4'-n-hexyl 4-cyanobiphenyl (6CB) and trans-p-n-octyloxy α-methyl p'-cyanophenyl cinnamate (8 OMCPC). The large dielectric anisotropy observed in them (see chapters III and IV) is due to the presence of C≡N along the long molecular axis. Both the samples wars synthesized in our chemistry laboratory. The nematic-isotropic transition temperature of 6CB was 29.1 °C and that of 8 OMCPC was 71.7 °C.

b. Method of measurement

The experimental set up used for the birefringence measurements is shown schematically in figure 6.2. A nicol prism was used to polarize \$h@light from *8* He-Ne laser (Spectra Physics, Model 132) at an angle of 45° to the field (electric or magnetic) direction. The phase retardation introduced in the sample was measured as a rotation of the plane of polarisation using a quarter-wave plate whose principal axes were inclined at an angle of 45° to the field direction. The $\lambda/4$ plate for $\lambda = 6328$ Å was cleaved from mica. The rotation was measured by means of a graduated analyser (Winkel-Zeiss) reading to an accuracy of 0.02°. When light passes through L cm of the sample the induced birefringence

$$\Delta n = \frac{\lambda R}{\pi L} ,$$

where R is the rotation measured in radians. The position of the minimum intensity was located using a

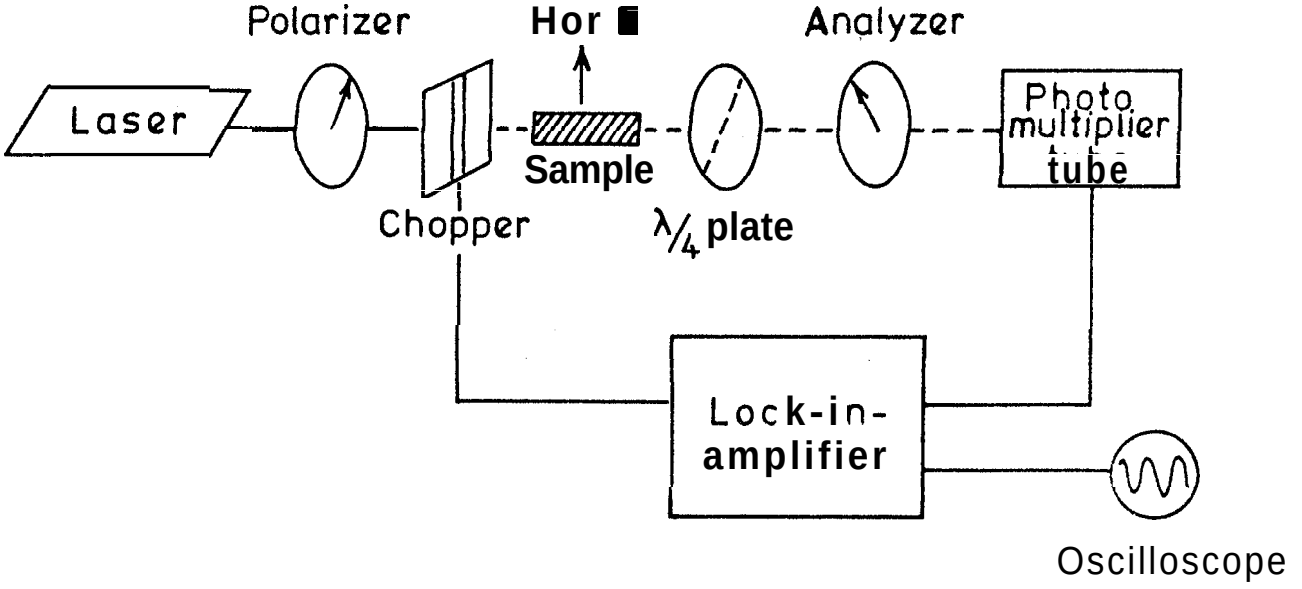


Figure 6.2

Schematic diagram showing the experimental set up used for the electric and magnetic birefringence measurements.

photomultiplier tube (Philips PW 4111) in conjunction with a lock-in-amplifier (Unipan-Selective Nanovoltmeter type 227, Homodyne Rectifier Voltmeter type 202B). For measuring $\Delta n_M$ the incident light was modulated using a chopper; an electronic chopper (American Time Products type TMC-L80) at 400 Hz was used in the case of 6CB and a variable speed chopper (Princeton Applied Research Model 192) at 500 Hz was used for 8 OMOPC. A 15 cm electromagnet (BDS Bangalore) was used at 40 mm pole separation. In $\Delta n_E$ measurements the AC electric field itself served as the modulation. A sine-wave generator (Orion-100640, Hungary) with a matched step-up transformer gave a maximum of 1 kV at 500 Hz. Since the induced birefringence is proportional to the square of the applied field, detection had to be dons at 1 kHz. The electrical conductivities of the samples were very low ($\sim 10^{-10}$ $ohm^{-1}$ $cm^{-1}$) and therefore the problems of electrohydrodynamic disturbance or heating of the sample did

not arise. The voltage applied was measured by an electronic multimeter (Philips PM 2400). The electrode separation was accurately measured on a comparator. The magnetic field was measured using a fluxmeter (Bell, USA). $\Delta n_E$ was measured at fields of 1.56, 2.34 and 3.125 kV/cm for 6CB and 2.98 and 3.92 kV/cm for 8 OMCPC. In the case of $\Delta n_M$ measurements the strengths of the magnetic field used were 5600 and 6900 Gauss for 6CB and 5600 and 6520 Gauss for 8 OMCPC.

c. Electric birefringence cell

The cell used for $\Delta n_E$ measurements of 6CB and 8 OMCPC is shown schematically in figure 6.3. It consisted of an optical cell of rectangular cross-section into which non-magnetic stainless steel electrodes were inserted with teflon spacers. The electrode assembly was held rigidly in position by two binding screws. The electrode separation was 0.32 cm for 6CB and 0.255 cm for 8 OMCPC. The length of the electrodes,

**Figure 6.3**

Schematic diagram of the cell used for electric birefringence measurements. 1. Optical cell 2. Non-magnetic stainless-steel electrodes 3. Teflon spacers 4. Glass windows in the heater 5. Chromel-alumel thermocouple 6. Teflon washer 7. Spring mounted studs 8. Nozzle 9. Binding screws.

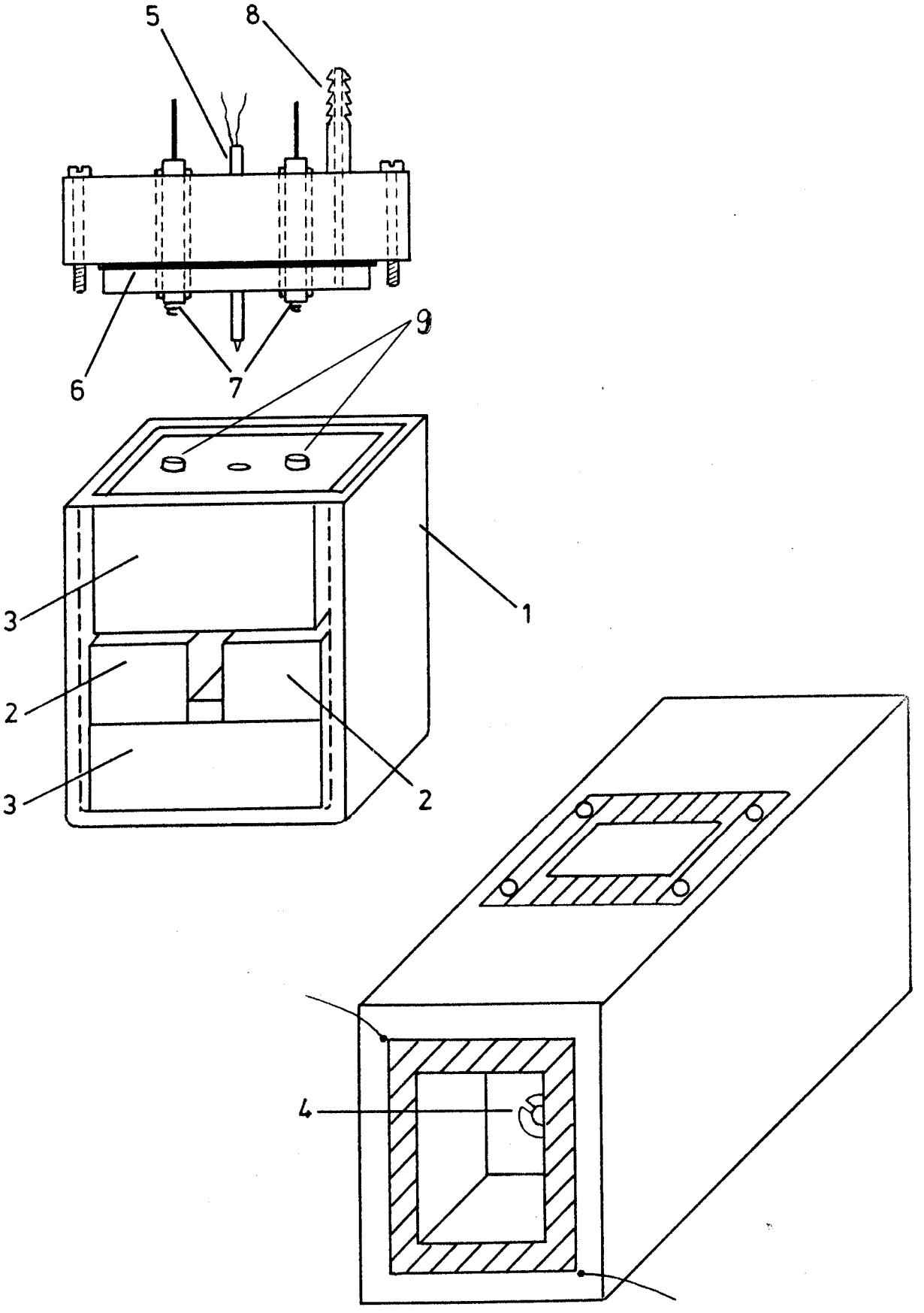
5
8
6
7
9
3
1
2
2
3
4

which was the effective optical path length,was 1 cm. The height of the electrodes was also 1 cm so that the light beam of 0.5 mm cross-section can be assumed to be passing through a uniform electric field.

The glass cell was enclosed in an electrically heated copper chamber provided with optically flat strain-free glass windows (see figure 6.3). The tempe- rature of the cell could be controlled to better than 0.05 °C. A chromel-alumel thermocouple, whose hot junction was positioned just above the top edge of the electrodes, was used to measure the sample temperature to an accuracy of 0.025 °C. The cell was completely isolated from the outside atmosphere once the lid with the teflon washer was screwed in. The stainless steel spring mounted studs in the lid made contact with the electrodes through the binding screws. The other end of the studs projected out of the top of the lid so that high voltage could be applied between them. The studs were insulated from the lid by teflon sleeves.

The nozzle provided in the lid served to evacuate the chamber and fill it with dry nitrogen. All the measurements were done with the sample in an atmosphere of nitrogen to prevent oxidation of the sample.

d. Magnetic birefringence cells

In order to measure $\Delta n_M$ to the same accuracy as $\Delta n_E$ it was necessary to increase the pathlength of the magnetic birefringence cell. (For example, in the case of 6OB, the rotations induced by the highest electric and magnetic fields used were 9.58 and 0.44 degrees/cm respectively at the same temperature.) In the case of 6OB the sample available was very little ($\sim$ 200 mg) and therefore a very narrow cell had to be designed. It consisted of a narrow teflon tube (figure 6.4a), of length 10.23 cm and internal diameter 1.5 mm, with a tight fitting copper jacket. The windows of the cell consisted of two optically flat strain free glass plates. Each window was secured to the cell by a copper

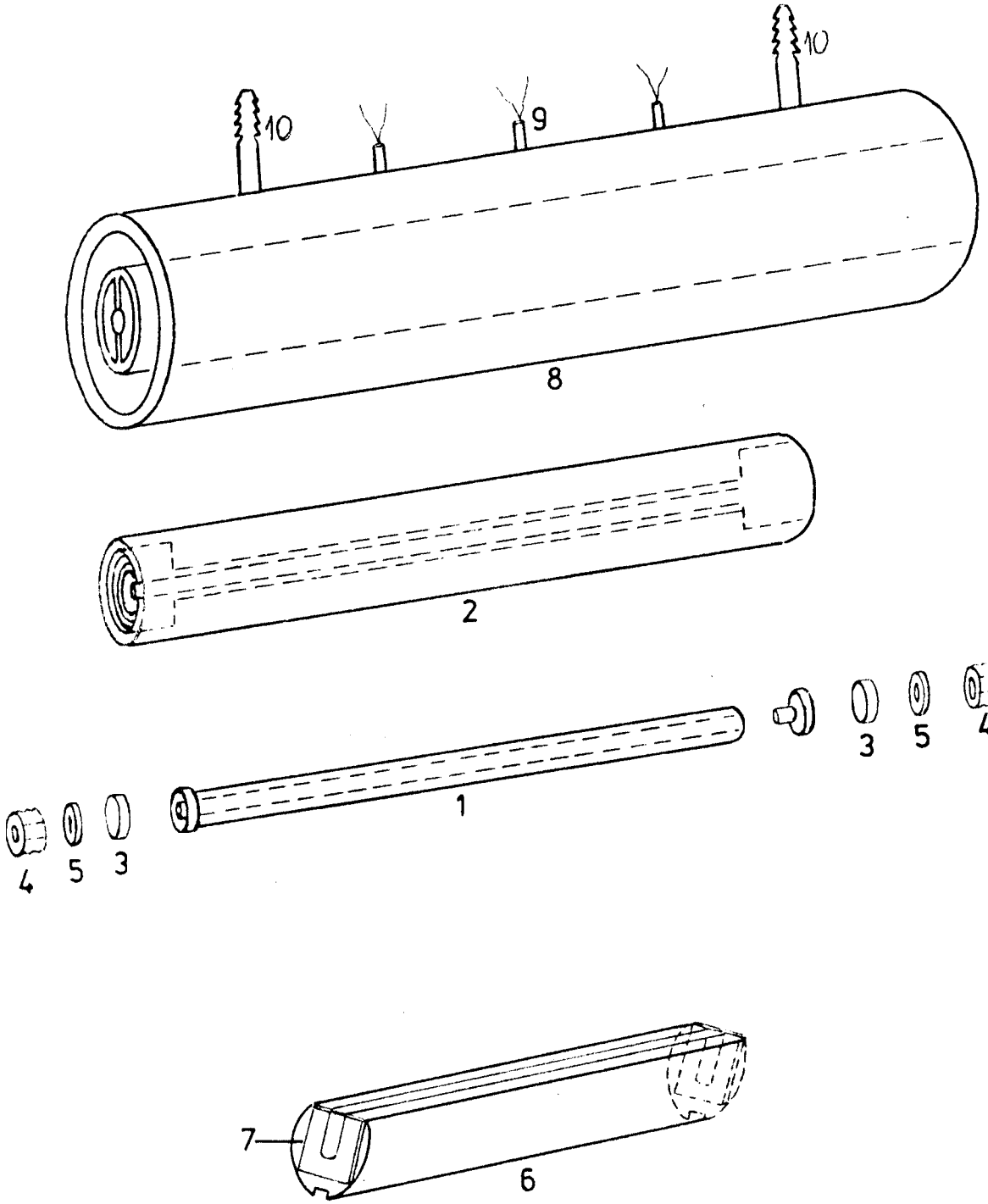


Figure 6.4: Schematic diagrams of the magnetic birefringence cells used for (a) 6CB and (b) 8 OMCPC. 1. Teflon tube 2. Copper jacket 3. Glass plates 4. Copper nuts 5. Teflon washers 6. Stainless-steel tubs 7. Glass windows 8. Heater 9. Thermocouples 10. Nozzles.

nut and a leak proof seal was achieved by using teflon washers between the glass plate and the nut. To begin with only one window was locked and the sample filled through the other end using a long and thin hypodermic needle and syringe. Once the tube was filled the other window was tightly secured taking care that no air bubble is introduced in the process.

8 OMCPC, being a solid at room temperature, could not be filled inside the teflon tube without air bubbles. Therefore a different type of cell had to be used for this compound. This cell (figure 6.4%) consisted of a 6.95 cm long non-magnetic stainless steel tube of internal diameter 3 mm. A 3 mm wide slot made along the length of the tuba helped in filling the sample in the cell. A guide was fixed in the heater so that the cell is always positioned with the slot at the top. Two optically flat strain *free* glass plates were fixed to the two ends of the tube using an epoxy (Epo-Tek H77) which could stand

temperatures up to 150 °C and which did not react with the sample.

The outer dimensions of the two magnetic birefringence cells were the same so that a common heater could be used for both of them. The heater was made of a copper tube (30 cm long) of large thermal mass over which nichrome wire was wound. The winding was insulated from the body of the heater by a sheet of mica. The cell was positioned at the centre of the heater using copper buffers. The heater was sealed by glass windows. The temperature of the sample could be accurately controlled by fine variations of the current through the nichrome wire. Three chromel-alumel thermocouples fixed in the heater were used to measure the temperature of the sample at different points and thereby ensured that there was no thermal gradient in the sample. Two nozzles were provided to flush the heater chamber with nitrogen before heating the sample.

All the cells were calibrated by measuring the Kerr constant and the Cotton-Mouton constant of freshly distilled nitrobenzene. The agreement between the measured and standard values of the constants was better than 2% which is therefore reckoned to be the absolute accuracy.

## Results and Discussion

According to equations (6.6) and (6.9) the birefringence ( $\Delta n_M$ or $\Delta n_E$) varies as the square of the field (magnetic or electric). Since the measured angle of rotation (R) is proportional *to* birefringence, we have plotted in figures 6.5 and 6.6 R versus $H^2$ and R versus $E^2$ respectively for 6CB at different temperatures. All of them are straight lines passing through the origin.

In figure 6.7 we have plotted both $\Delta n_M$ and $\Delta n_E$ as functions of temperature *for* 6CB measured at the highest fields. Both exhibit very strong anamolies.

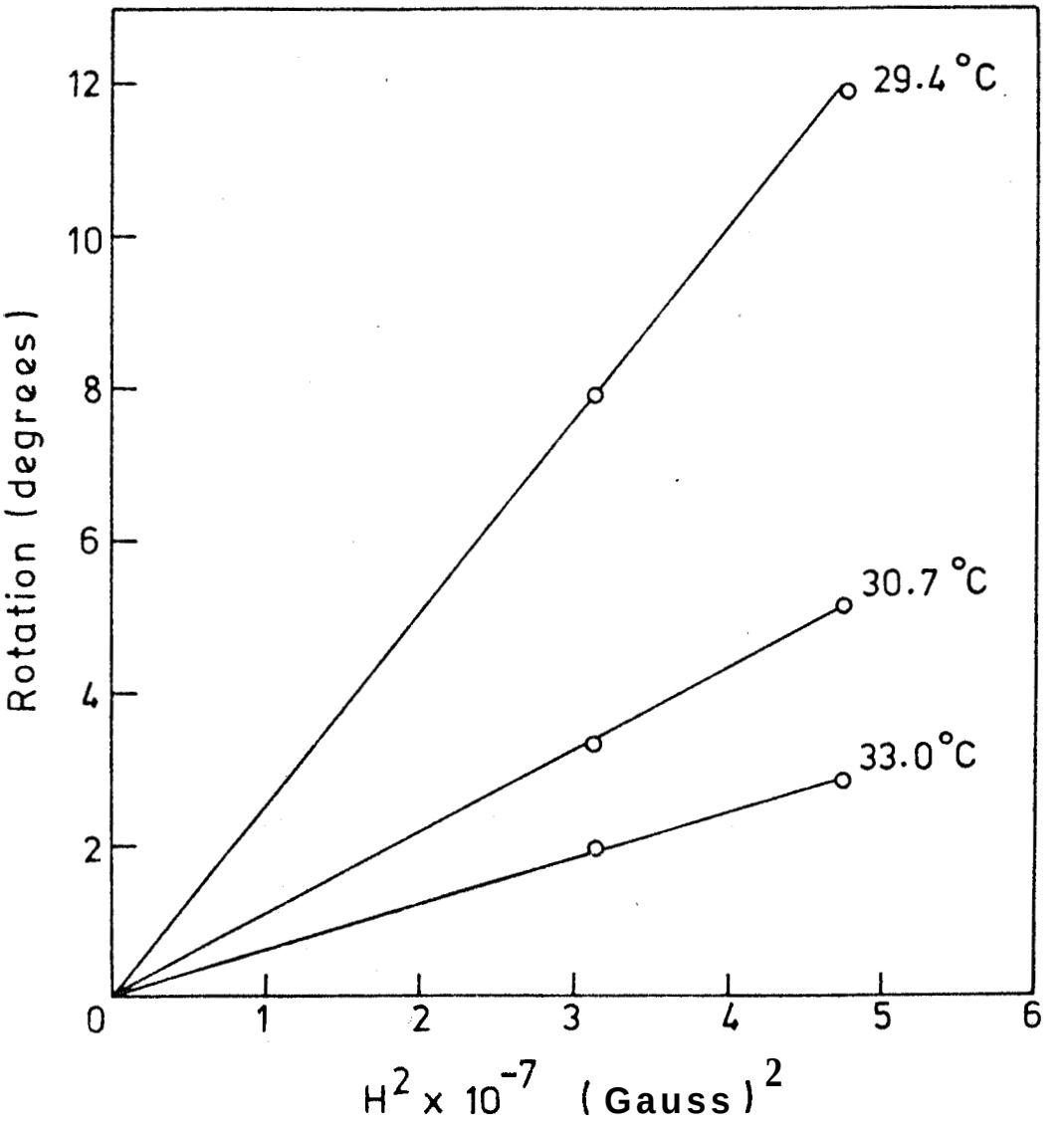


Figure 6.5

Rotation versus square of the magnetic field at different temperatures for 603.

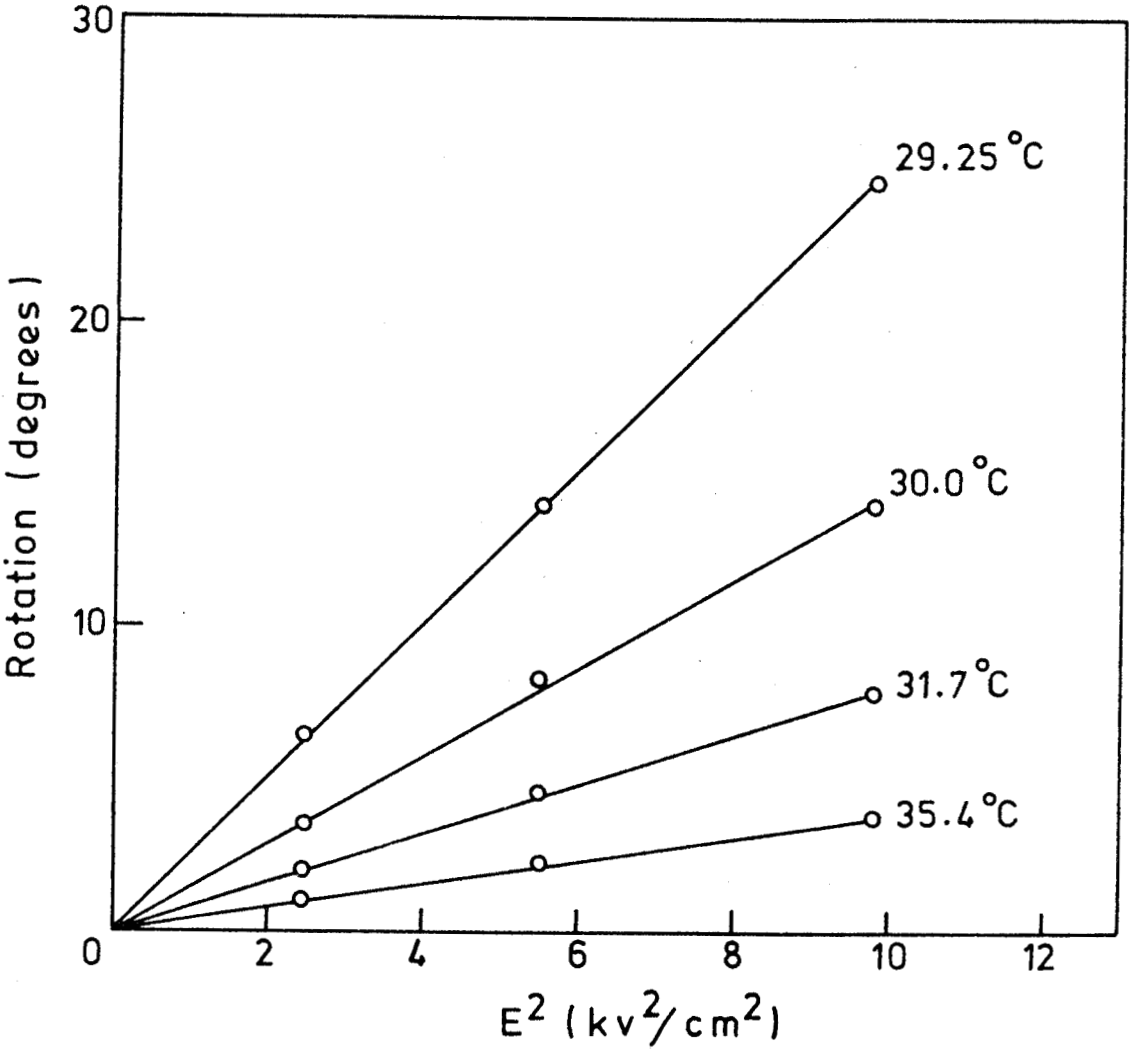


**Figure 6.6**

**Rotation versus square of the electric field at different temperatures for 6CB.**

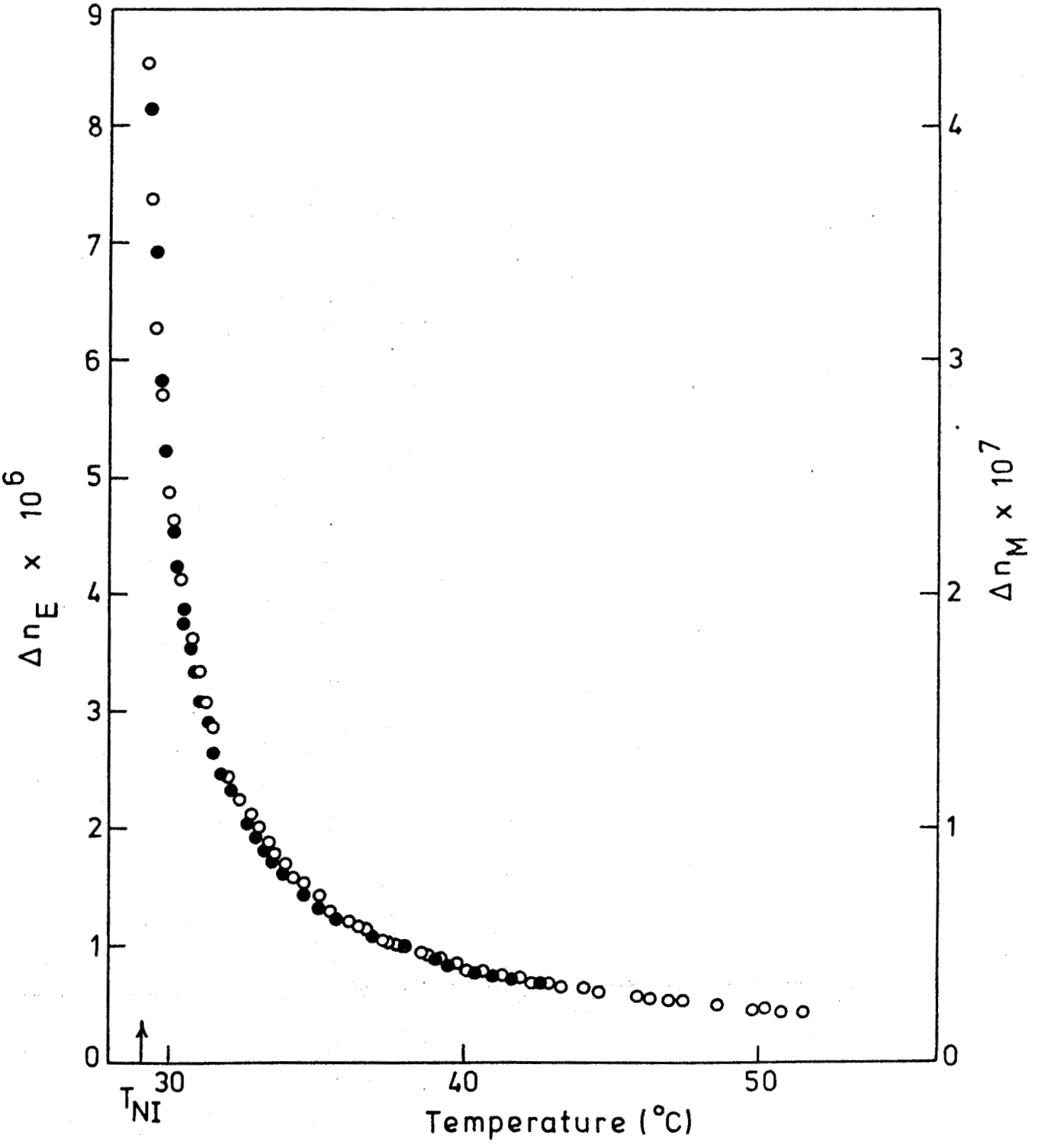


**Figure 6.7**: Magnetic (●) and electric birefringence (○) as functions of temperature for 6CB. The measuring fields were H = 6900 Gauss and E = 3.125 kV/cm.

$\Delta n_E$ was measured over a temperature range of about 25 °C. However $\Delta n_M$ could be measured only up to 14 °C above $T_{NI}$ since at this temperature the variation of $\Delta n_M$ became comparable to the accuracy of the instrument. In both $\Delta n_E$ and $\Delta n_M$ measurements, rotations were measured at temperatures as close as 0.1 °C to $T_{NI}$.

In figure 6.8 we have shown the variation of the inverse of $\Delta n_M$ with temperature for 6OB for the two field strengths. The least squares fit to the data points are straight lines which on extrapolation give the hypothetical second order transition point $T^*$ at 28°C. The fact that $(\Delta n_M)^{-1}$ versus T is a straight line implies that the critical exponent is unity.

The inverse of the electric birefringence as a function of temperature is shown in figure 6.9. The variation is linear for all the three field strengths establishing the $(T - T^*)^{-1}$ dependence of $\Delta n_E$ also. On extrapolation all the lines meet at the same $T^*$

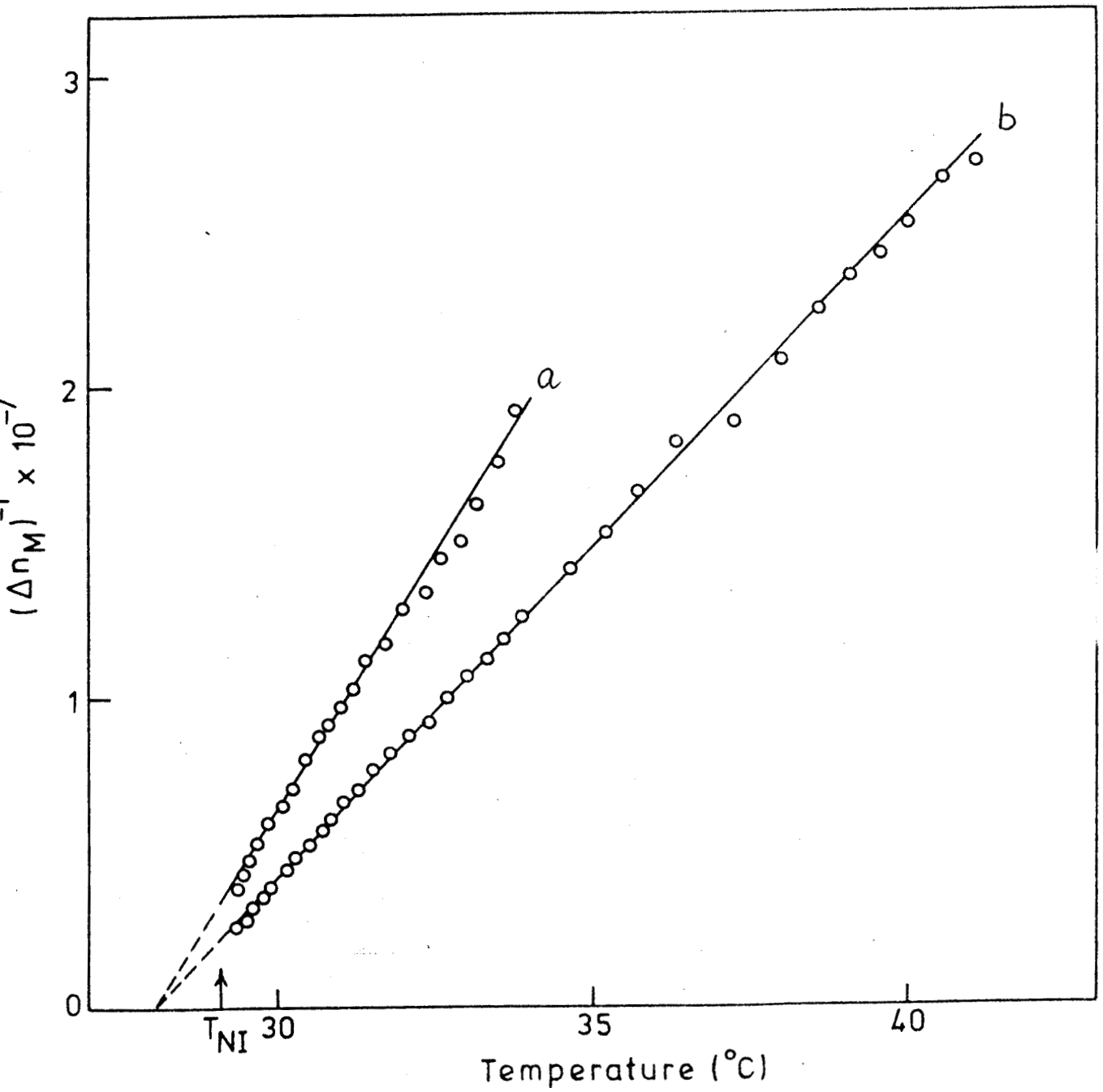


**Figure 6.8**

$(\Delta n_M)^{-1}$ versus temperature for 6CB. H = 5600 (a) and 6900 (b) Gauss. ($T_{NI}$ = 29.1 °C; $T^*$ = 28 °C).

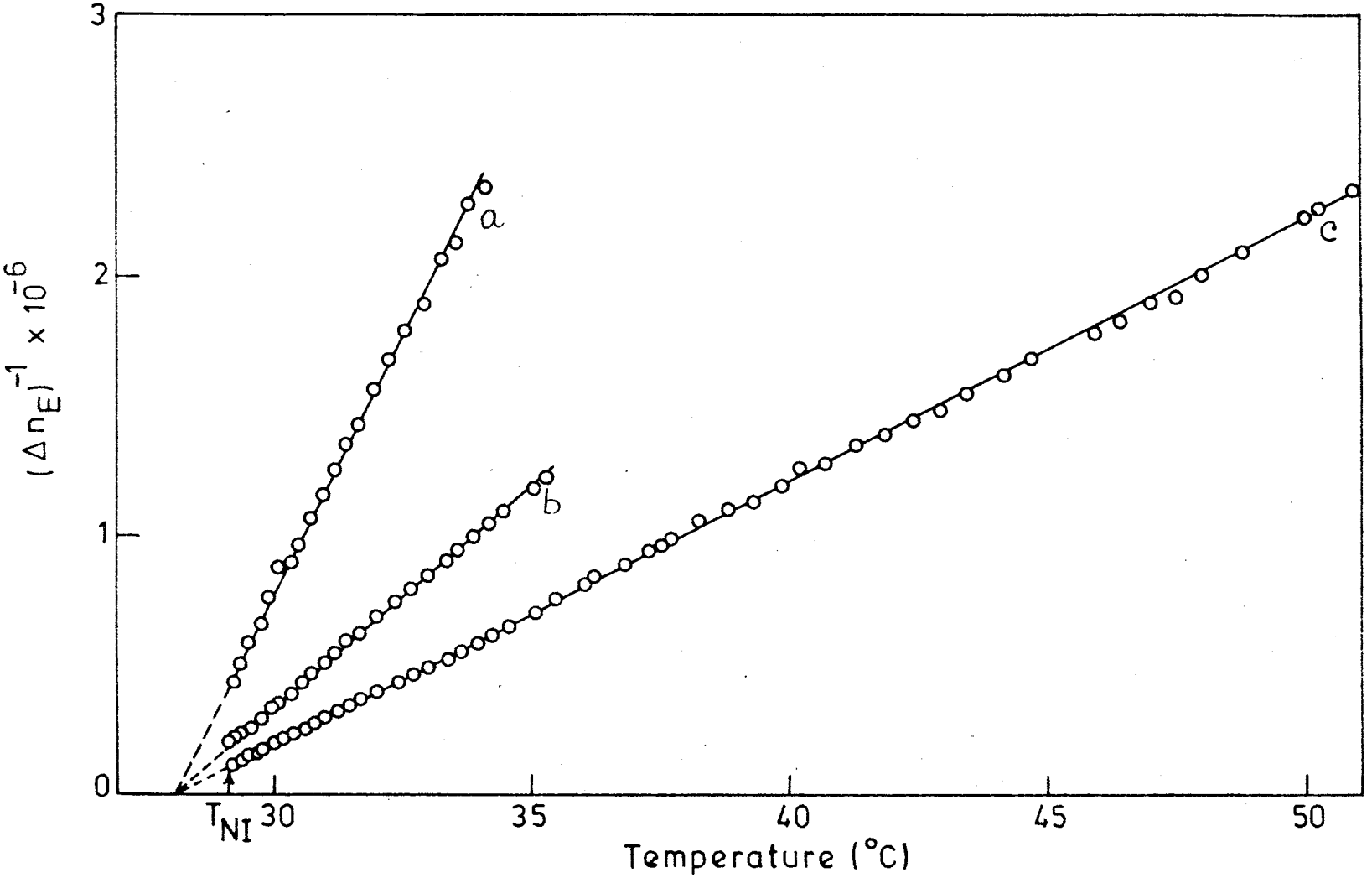


**Figure 6.9**

Inverse of $\Delta n_E$ versus temperature for 6CB. E = 1.56 (a), 2.34 (b) and 3.125 (c) kV/cm. ($T_{NI}$ = 29.1 °C, $T^*$ = 28 °C).

(28.0 °C). We notice that both $\Delta n_M$ and $\Delta n_E$ give identical values of $T^*$ and $T_{NI} - T^*$ (1.1 °C).

Exactly similar results were obtained for 8 OMCPC also. In figures 6.10 and 6.11 we have shown the quadratic dependence of the rotation on magnetic and electric fields. $\Delta n_M$ could be measured only up to 10 °C above $T_{NI}$ while $\Delta n_E$ was measured over a range of 20 °C. The variation of $\Delta n_M$ and $\Delta n_E$ with temperature in shown in figure 6.12. The inverse dependence of ~~both~~ $\Delta n_M$ and $\Delta n_E$ on temperature are shown in figures 6.13 and 6.14 with $T^* = 70.3$ °C and $T_{NI} - T^* = 1.4$ °C.

It has been experimentally well established[2,6] that $\Delta n_M$ exhibits a $(T - T^*)^{-1}$ dependence. On the other hand, $\Delta n_E$ of the few compounds that had been studied[10,13-15] did not help to draw any definite conclusion on the nature of its temperature dependence. PAA[10] showed a reversal in the sign of $\Delta n_E$ a few degrees

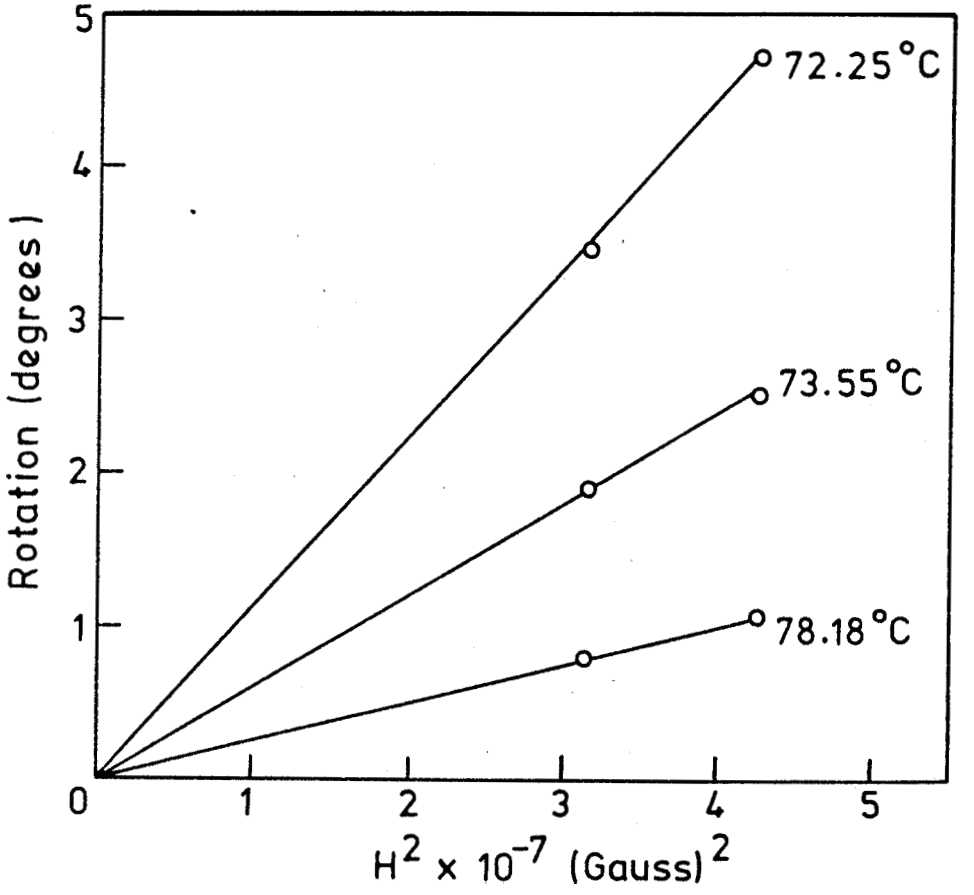


**Figure 6.10**

Rotation versus square of the magnetic field at different temperatures for 8 OMCPC.

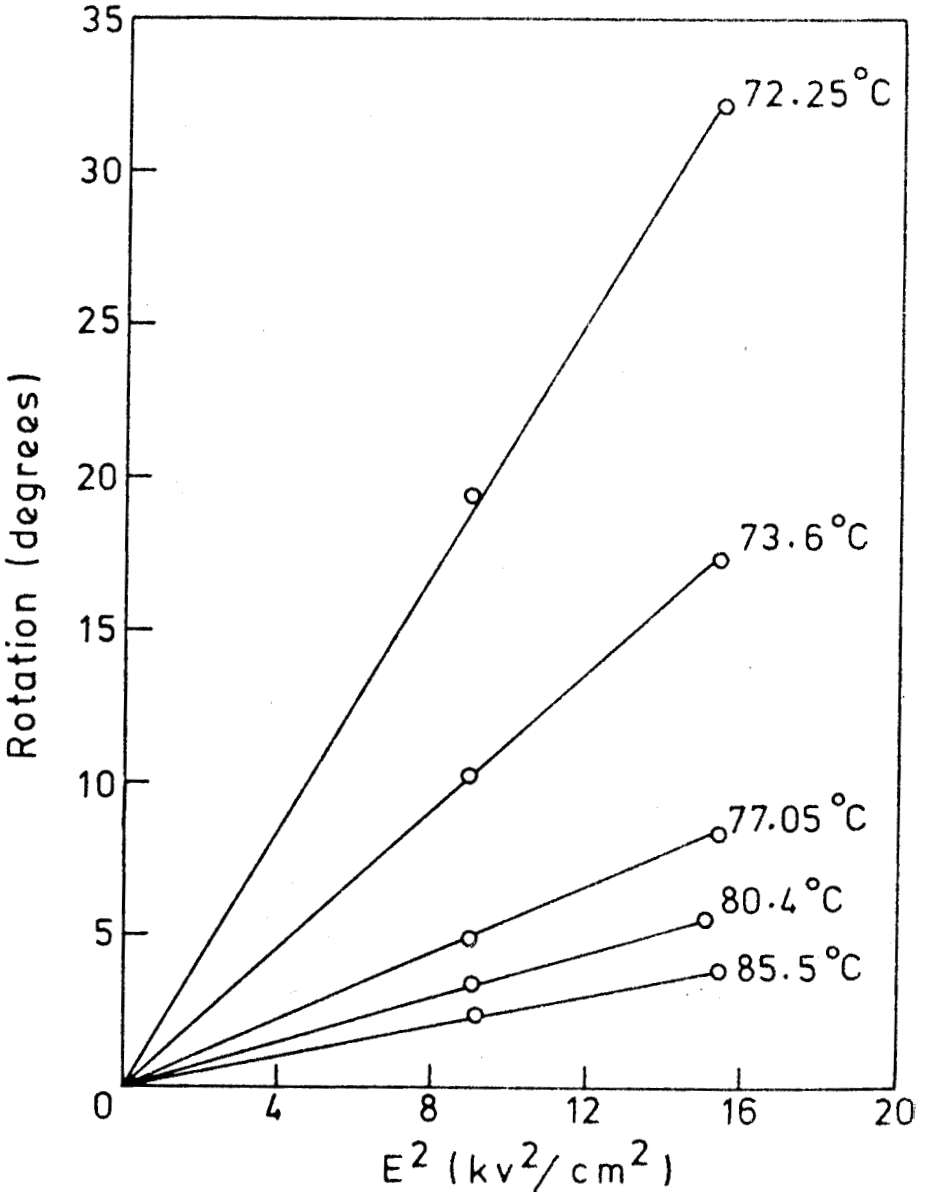


**Figure 6.11**

**Rotation versus square of the electric field at different temperatures for 8 OMCPC.**

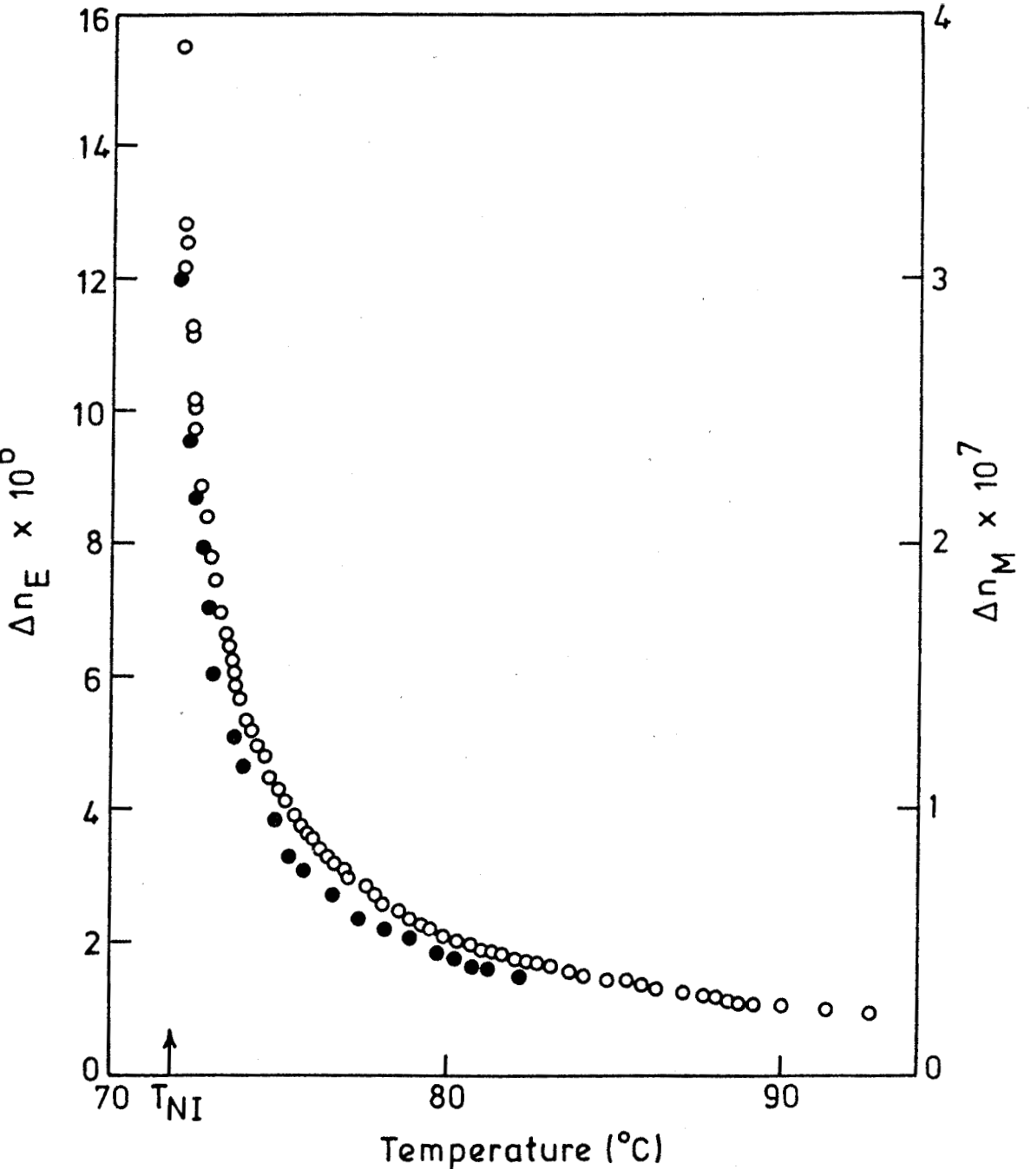


**Figure 6.12**

Magnetic (●) and electric birefringence (○) as functions of temperature *for 8* OMCPC. The measuring fields were H = 6520 Gauss and E = 3.92 kV/cm.

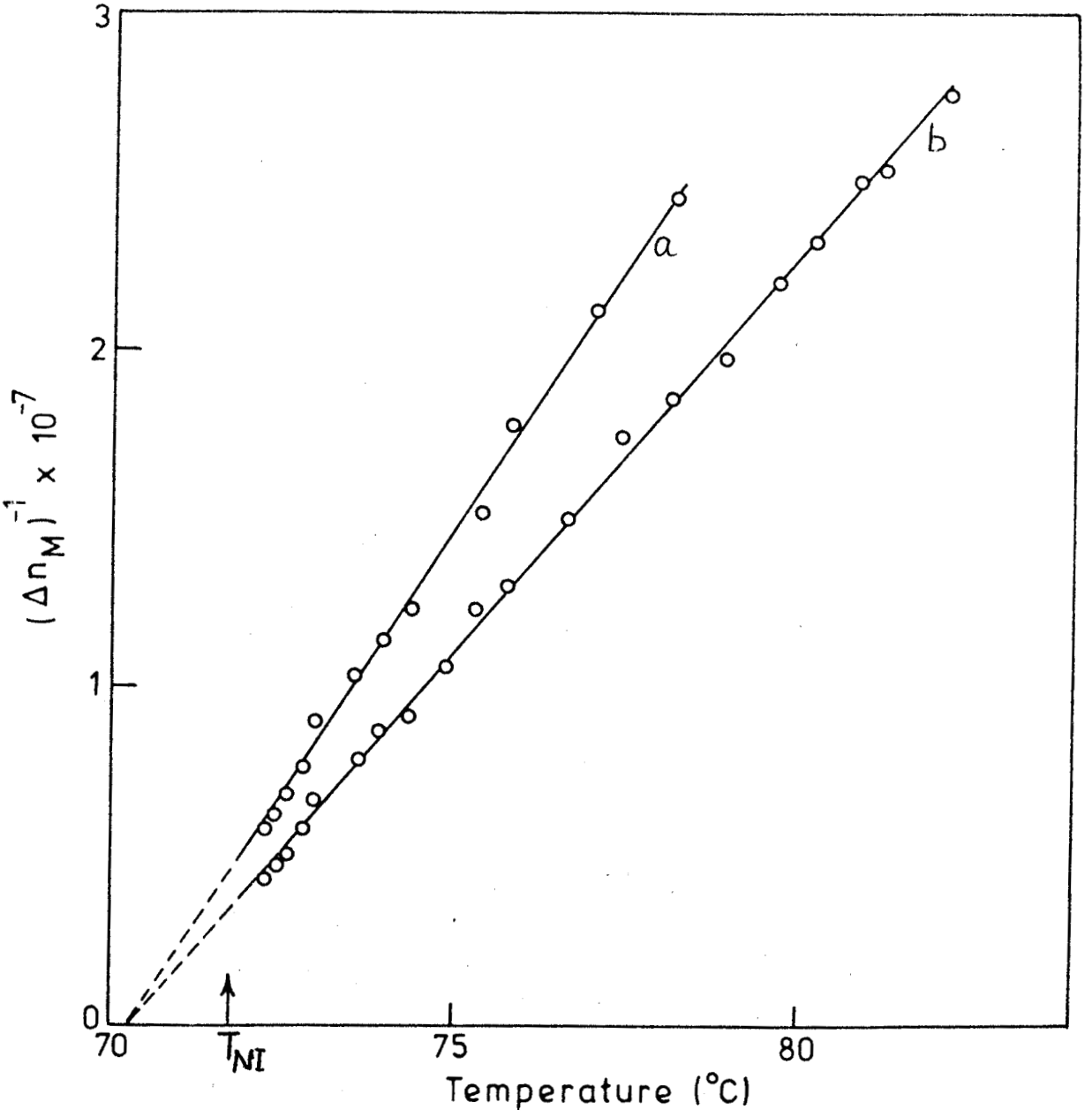


**Figure 6.13**

Inverse of $\Delta n_M$ versus temperature for 8 OMCPC.
H = 5600 (a) and 6520 (b) Gauss. ($T_{NI}$ = 71.7 °C, $T^*$ = 70.3 °C)

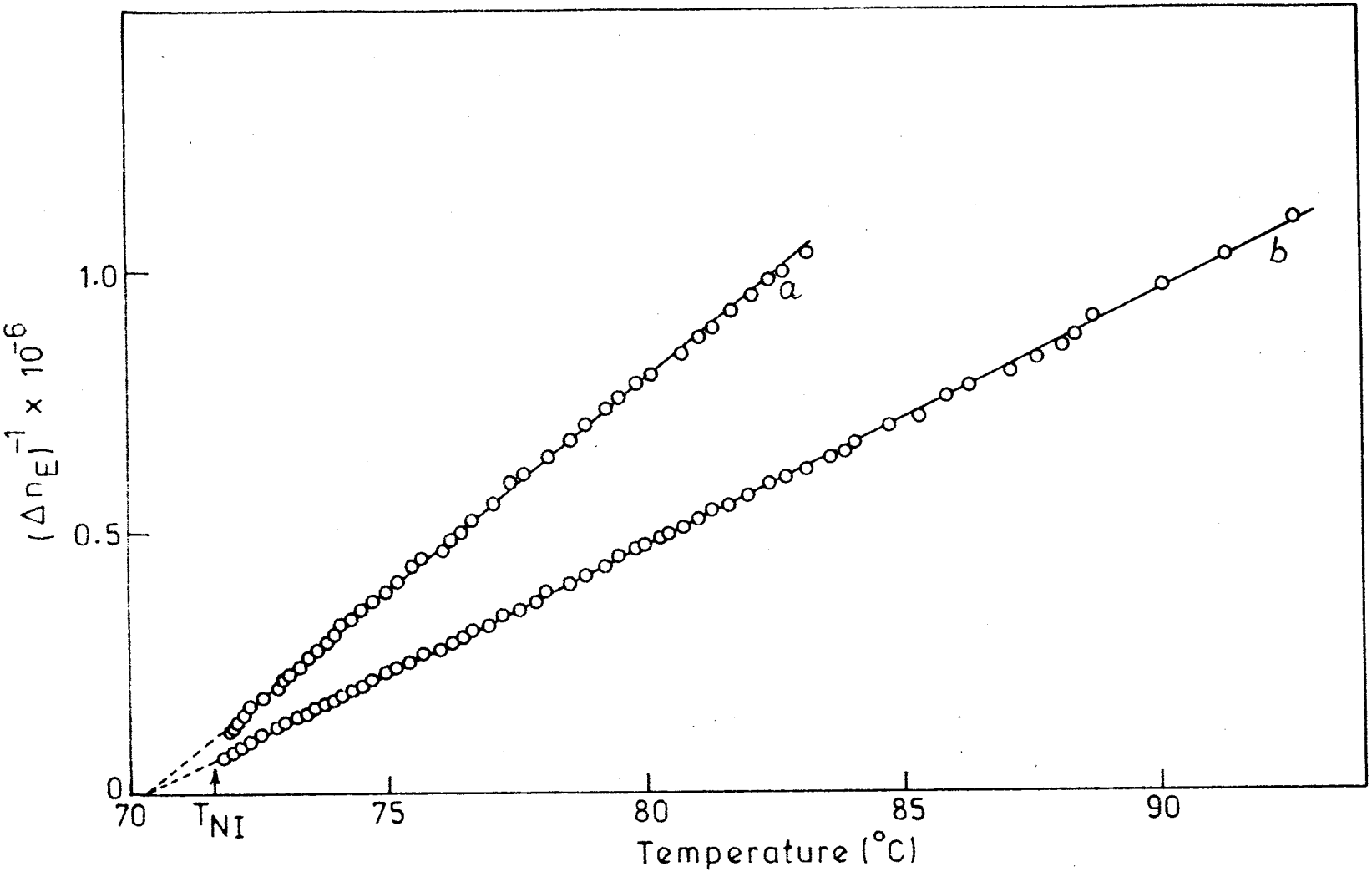


**Figure 6.14**

Inverse of $\Delta n_E$ versus temperature for 8 OMCPC. E = 2.98 (a) and 3.92 (b) kV/cm. ($T_{NI}$ = 71.7 °C, $T^*$ = 70.3 °C).

above $T_{NI}$. The first measurements on p-methoxy benzylidene p'-butyl aniline was by Filippini.[13] Because of the low purity of the sample $T_{NI}$ was changing continuously. As a result $T^*$ and hence the exponent could not be determined. However subsequent measurements[15,16] on purer samples of MBBA gave a $(T - T^*)^{-1}$ dependence. Schadt and Helfrich[14] measured the Kerr constant in some nitrile compounds with strong positive dielectric anisotropy and reported that the temperature dependence of $\Delta n_E$ is expressible as $(T - T_{NI})^{-\gamma}$ where $\gamma$ ranged between 0.5-0.7, the difference $(T_{NI} - T^*)$ being very small ($\sim$ 0.2 °C). They also remarked that it would be of interest to see if $\Delta n_M$ of such compounds also exhibit a slower variation with temperature. However our measurements on 6CB and 8 OMCPC have established unambiguously that both $\Delta n_M$ and $\Delta n_E$ of strongly positive materials yield $\gamma = 1$. Filippini and Poggi[17] have subsequently measured $\Delta n_M$ and $\Delta n_E$ for 5CB and

7CB also. From a log-log plot of $\Delta n_M$ and $\Delta n_E$ versus $(T - T^*)$ the slope of which gives the exponent, they obtain a value of 1 for $\gamma$ over a wide range of temperature. However they obtain a slower variation for temperatures beyond $T_{NI}$ + 20 °C. We did not find any such change of slope for 6CB in the temperature range ($\sim$ 22 °C) covered by us. Thus it is now well established that both $\Delta n_M$ and $\Delta n_E$ in the isotropic phase of a nematic obey the Landau type of description of the nematic-isotropic transition.

## References


1. J. Zadoc-Kahn, Compt. Rend., 191, 1002 (1930).
2. G. Foex, Trans. Faraday Soc., 29, 958 (1933).
3. P. G. de Gennes, Mol. Cryst. Liquid Cryst. 12, 193 (1971).
4. L.D. Landau and E.M. Lifshitz, Statistical Physics, 2nd Edition, Pergamon (1969).
5. J.W. Beams, Rev. Mod. Phys. 4, 133 (1932).
6. T.W. Stinson and J.D. Litster, Phys.Rev.Letters 25, 503 (1970).
7. A. Saupe and W. Maier, Z. Naturforsch. 16a, 816 (1961).
8. H. Gasparoux, B. Regaya and J. Prost, Compt. Rend. 272B, 1168 (1971).
9. N.V. Madhusudana and S. Chandrasekhar, Liquid Crystals and Ordered Fluids, Vol. 2, Eds. J.F. Johnson and R.S. Porter, p. 657, Plenum (1974).
10. V.N. Tsvetkov and E.T. Ryumtsev, Soviet Phys. Crystallogr. 13, 225 (1968).
11. W. Maier and G. Meier, Z.Naturforsch. 16a, 470 (1961).

12. N.V. Madhusudana and S. Chandrasekhar, Proc. Int. Liquid Cryst. Conf., Bangalore, 1973; Pramana Suppl. 1, 57.

13. J.C. Filippini, C.R.Hebd.Sean.Acad.Sci. B275, 349 (1972).

14. M. Schadt and W. Helfrich, Mol. Cryst. Liquid Cryst. 17, 355 (1972).

15. A.R. Johnston, J. Appl. Phys. 44, 2971 (1973).

16. J.C. Filippini and Y. Poggi, J.Physique 36, C1-137 (1975).

17. J.C. Filippini and Y. Poggi, J.Physique 37, L-17 (1976).

# CHAPTER VII

## PRESSURE DEPENDENCE OF THE PITCH NEAR THE SMECTIC A-CHOLESTERIC TRANSITION POINT

In most pure cholesterics the pitch is a slowly decreasing function of temperature. Keating[1] has given a theory of the cholesteric twist in analogy with the thermal expansion in crystals. Assuming anharmonic angular oscillations of the molecules about the helical axis, the mean angle between successive layers

$$\langle\theta\rangle = AkT/2I\omega_0^4 ,$$

where A is the coefficient of the cubic anharmonicity term, $\omega_0$ the angular frequency and I the moment of inertia of the molecule. Since the pitch is proportional to $1/\langle\theta\rangle$ one expects a slight 'red shift' in the wavelength of maximum reflection[2] $\lambda_R$ with decrease of temperature. However if the cholesteric phase is

preceded by a smectic A phase at lower temperature the pitch increases very rapidly as the sample is cooled to the smectic A-cholesteric transition point.[3] This is due to the growth of smectic like clusters in the cholesteric phase. de Gennes[4] used a Landau type of phenomenological model to describe the critical divergence of the twist elastic constant ($k_{22}$) near a smectic A-nematic (or cholesteric) transition point due to the build up of smectic-like short range order. Since the cholesteric pitch P is related to $k_{22}$,[5] we can express P in the form

$$P = P_0 + A(T - T_c)^{-\nu} , \qquad (7.1)$$

where $P_0$ is the intrinsic pitch in the absence of the smectic-like correlations and $T_c$ is the apparent second order smectic A-cholesteric transition point. Invoking the analogy with superfluids de Gennes predicted the value of the critical exponent $\nu$ as 2/3.

Pindak Huang and Ho[6] have investigated in some detail the critical divergence of the pitch in cholesteryl

nonanoate which shows a smectic A phase below 74 °C. They determined the intrinsic pitch and its temperature dependence by studying mixtures of cholesteryl nonanoate (CN) with cholesteryl chloride (CC) and extrapolating to zero concentration of CC. Their experiment yields a value of 0.675 ± 0.025 for $\nu$ which is in good agreement with the theoretical prediction.

Pollmann and coworkers[8-11] have measured the pitch as a function of pressure far a number of cholesterics having a smectic A phase at lower temperatures. They showed that the pitch increases rapidly with pressure, approaching infinity at a critical pressure $p_c$ whose value depends on the temperature of the sample. The cholesterics studied by them are cholesteryl oleyl carbonate (COO),[10,11] cholesteryl myristate (CM)[10] and mixtures[8,9] of COC and CC. The pitch versus pressure plots for one of them (COC/CC =

83.0/17.0 mole %) at different temperatures are reproduced in figure 7.1.

The experiments were done by keeping the temperature of the sample ($T_S$) constant in the cholesteric phase. The application of pressure raises $T_c$ so that the pitch exhibits a critical divergence as $T_c$ approaches $T_S$. The critical pressure $p_c$ is that pressure at which $T_c = T_S$.

We have shown from a simple calculation that the observed critical divergence of the pitch with pressure is indeed to be expected from theoretical considerations. In pure COC and CN, $T_c$ increases linearly with pressure[12,13] to a good approximation. Assuming that the same type of linear variation is present in the mixtures also, at any given temperature T, (7.1) may be expressed as

$$P - P_0 = B(p_c - p)^{-\gamma}. \qquad (7.2)$$

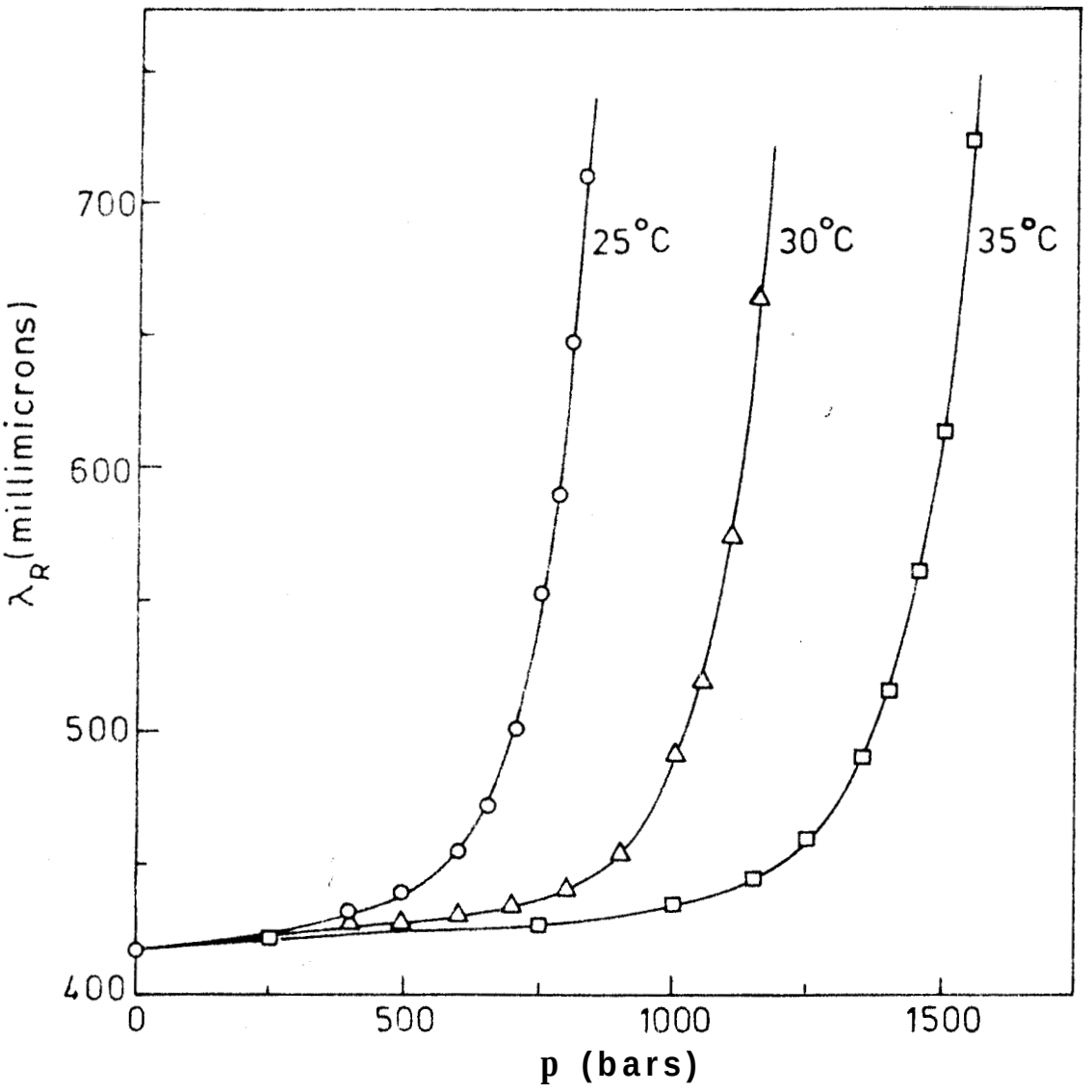


**Figure 7.1**

Wavelength of maximum reflection versus pressure for a mixture of cholesteryl oleyl carbonate (COC) and cholesteryl chloride (CC) at different temperatures. COC/CC = 83.0/170 mole %. (after Pollmann and Stegemeyer[9])

By fitting the experimental data of Pollmann and coworkers to this equation we *hare* evaluated $\nu$ . In all the calculations the wavelength of maximum reflection is used instead of the cholesteric pitch (or, in other words, we neglect the small change in the refractive index with pressure and wavelength). With the data available it was not possible to estimate the intrinsic pitch $P_0$ in the absence of the smectic phase. However, the dependence of $P_0$ on temperature and pressure may be expected to be quite small and thus we may justifiably neglect its variation in tho small range of interest near $p_c$ and write

$$\frac{\partial(P - P_0)}{\partial p} \approx \frac{\partial P}{\partial p} = B\nu(p_c - p)^{-\nu-1} . \quad (7.3)$$

We have estimated $\partial P/\partial p$ from the experimental curves of COO at two temperatures (59.6 °C and 64.3 °C), of ON at 115 °C and of three compositions of a mixture of COO and CC [(i) COC/CC = 83.0/17.0 mole % at 25 °C,

30 °C and 35 °C; (ii) COC/CC = 80.1/19.9 mole % at room temperature, and (iii) COC/CC = 78.0/22.0 mole % at 25 °C, 30 °C and 35 °C].

A log-log plot of $\partial P/\partial p$ versus $(p_c - p)$ for all these compounds (figures 7.2-7.6) is fairly linear in the vicinity of $p_c$ giving a value for $\nu$ between 0.68 and 0.71 (see table 7.1) in good agreement with de Gennes model. This simple calculation explains the rapid increase of the pitch with pressure as due to the build up of smectic like short range order in the cholesteric phase.

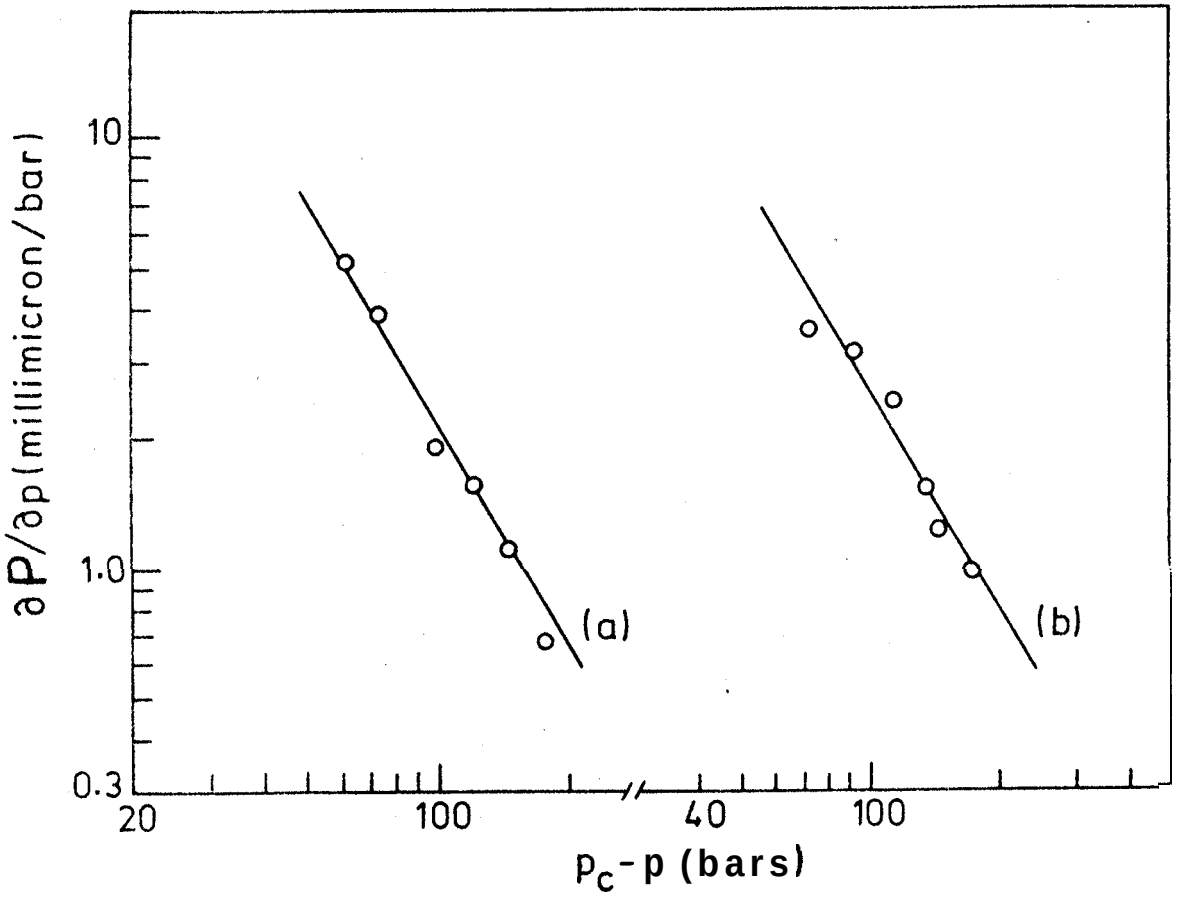


**Figure 7.2**

Log-log plot of $\partial P/\partial p$ versus $(p_o - p)$ for COC at (a) 59.6 °C ($p_o$ = 1960 barer) and (b) 64.3 °C ($p_o$ = 2266 bars).

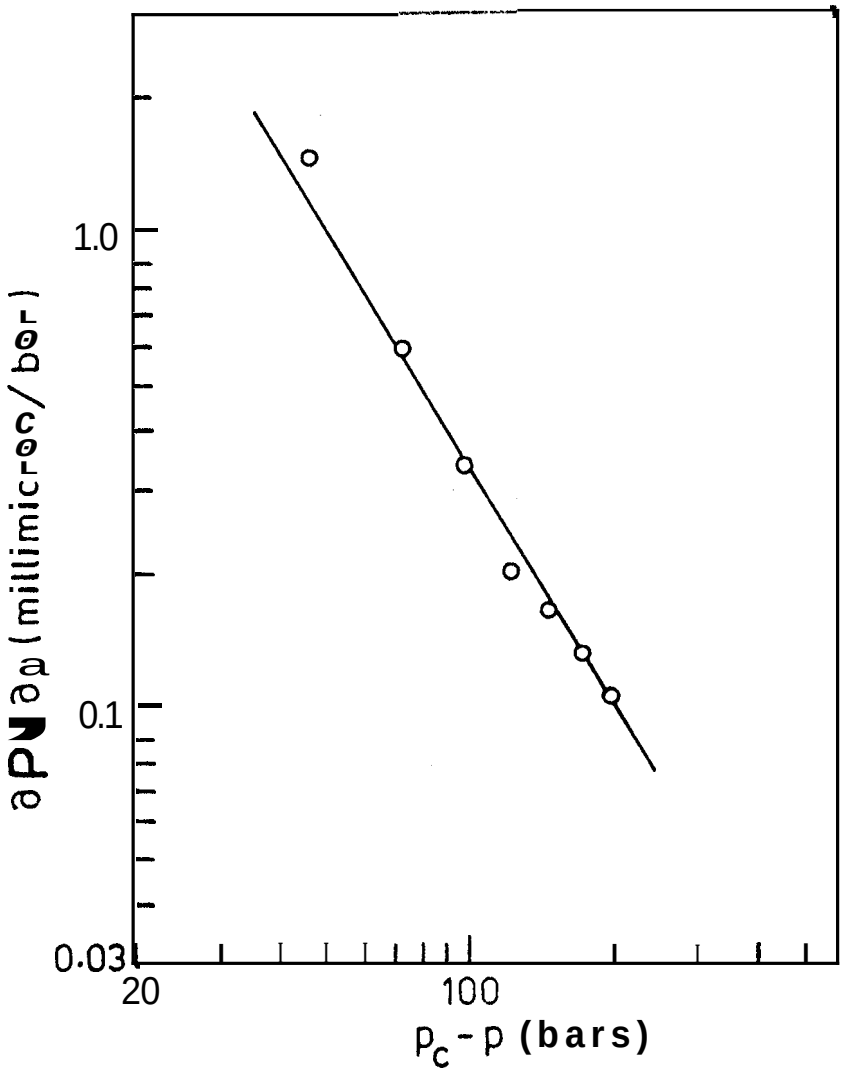


**Figure 7.3**

**Log-log plot of $\partial P/\partial p$ versus $(p_c - p)$ for cholesteryl myristate (CM) at 115°C ($p_c$ = 1570 bars).**

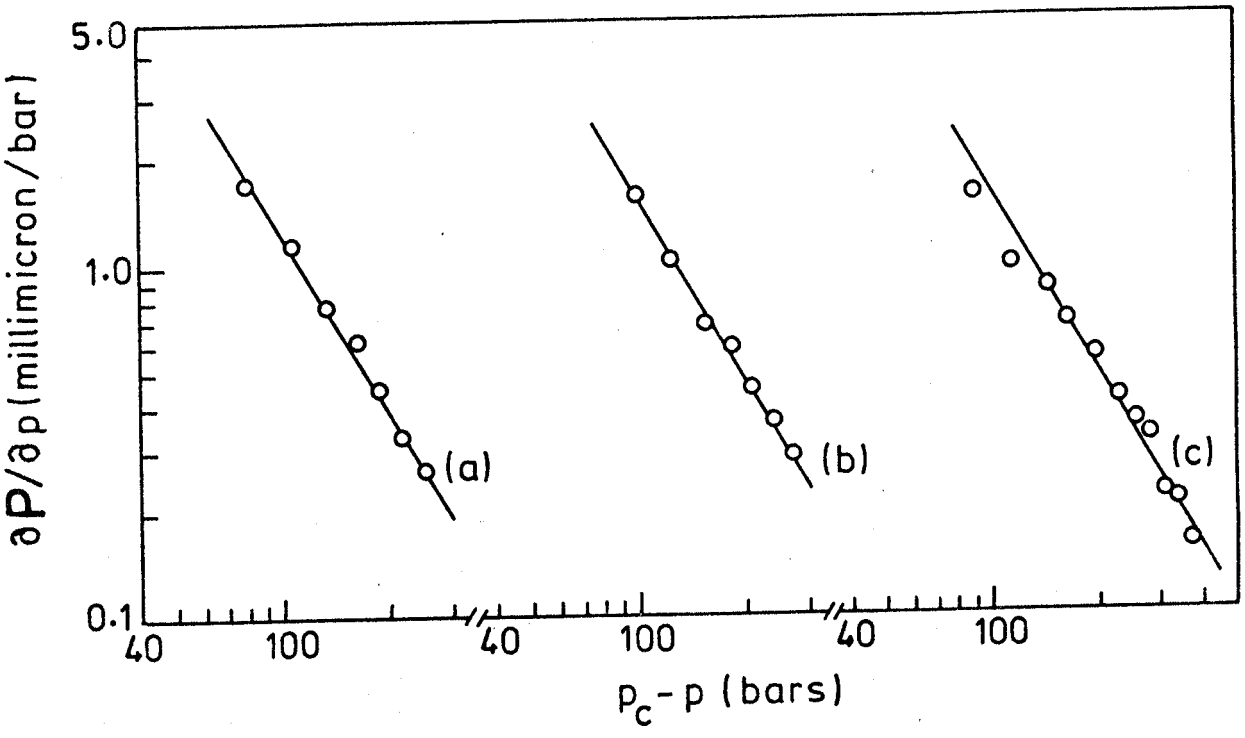


**Figure 7.4**

Log-log plot of $\partial P/\partial p$ versus $(p_c - p)$ for a mixture of COC and CC (83.0/17.0 mole %) at (a) 25 °C ($p_c$ = 850 bars) (b) 30 °C ($p_c$ = 1200 bars) and (c) 35 °C ($p_c$ = 1575 bars).

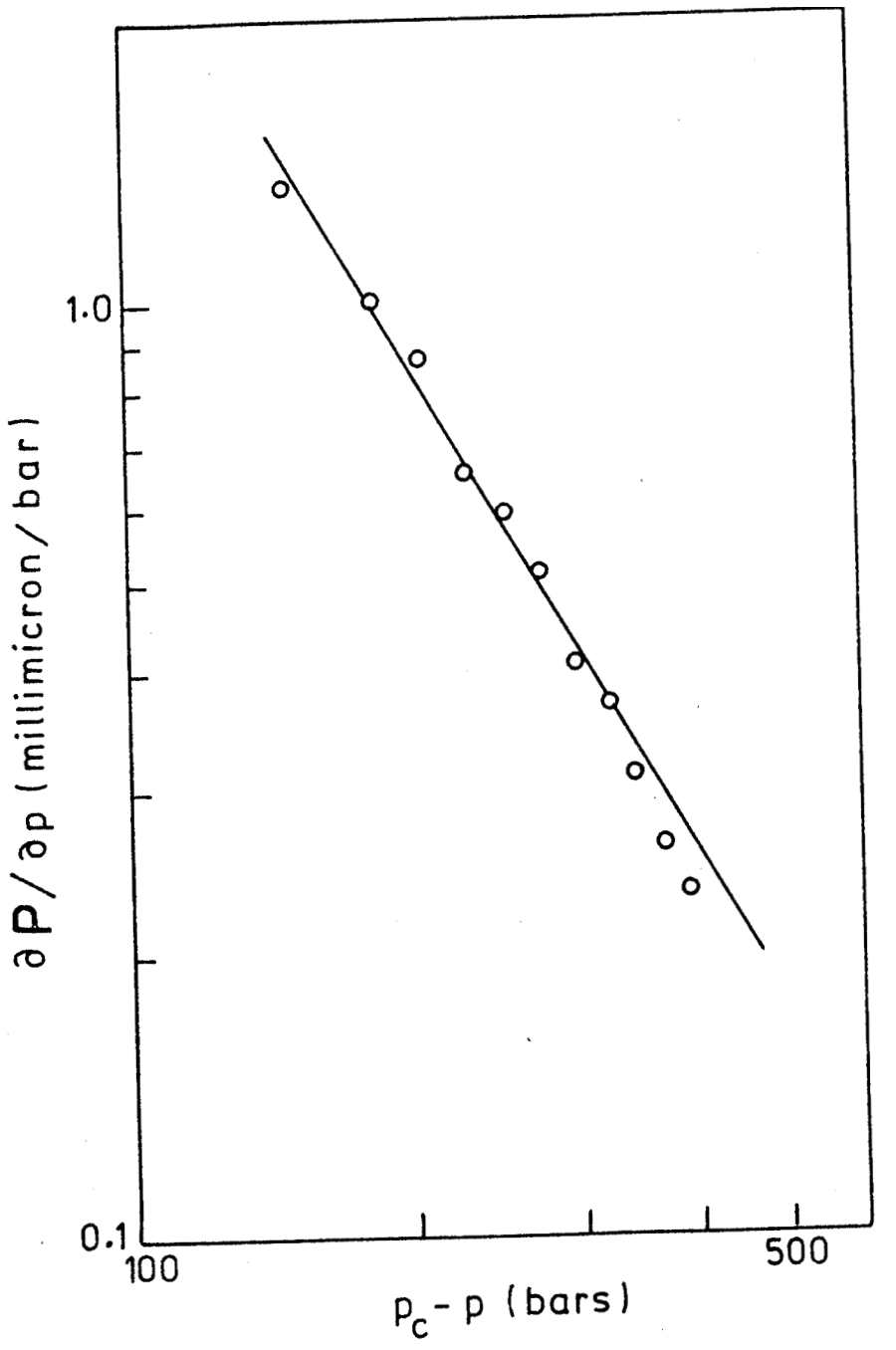


Figure 7.5

Log-log plot of $\partial P/\partial p$ versus $(p_c - p)$ for a mixture of COC and CC (80.1/19.9 mole %). $p_c$ = 900 bars

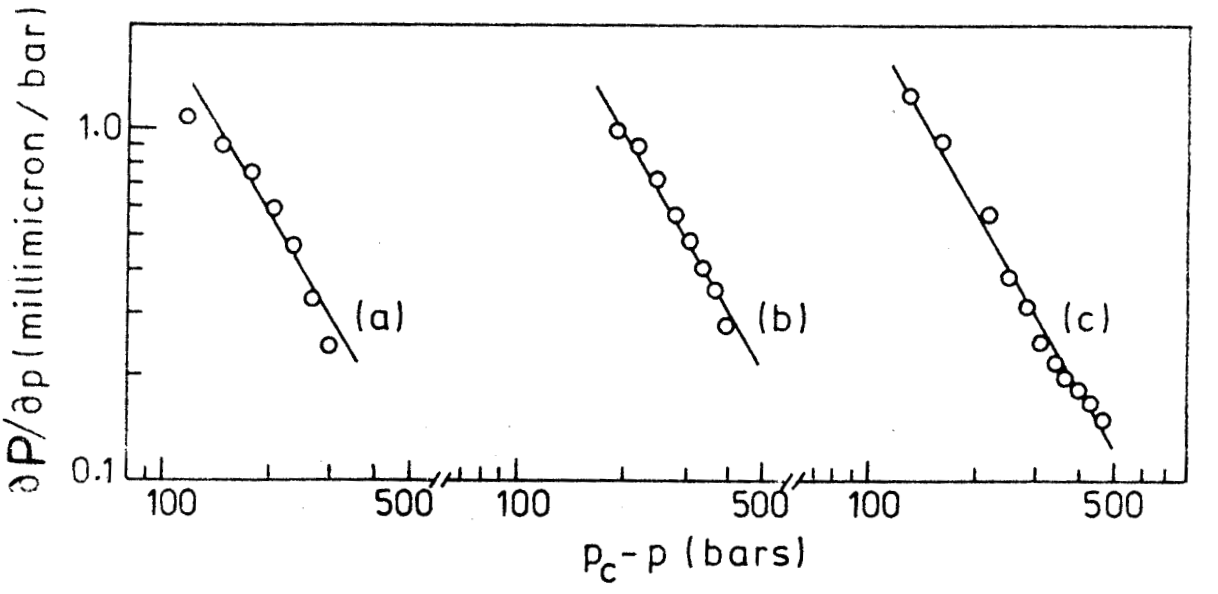


**Figure 7.6**

Log-log plot of $\partial P/\partial p$ versus $(p_c - p)$ for a mixture of CCC and CO (78.0/22.0 mole %) at (a) 25°C ($p_c$ = 1200 bars) (b) 30°C ($p_c$ 1650 bars) and (c) 35°C ($p_c$ = 2090 bars).

**Table 7.1:** The value of critical exponent $\nu$ for cholesterics

| Compound | Temperature (°C) | $\nu$ |
|---|---|---|
| OOO | 59.6 | 0.70 |
| | 64.3 | 0.71 |
| ON | 115.0 | 0.68 |
| OOO/OO = 83/17 mole % | 25.0 | 0.69 |
| | 30.0 | 0.71 |
| | 35.0 | 0.71 |
| OOO/OO = 80.1/19.9 mole % | - | 0.70 |
| OOO/OO = 78/22 mole % | 25.0 | 0.68 |
| | 30.0 | 0.70 |
| | 35.0 | 0.70 |

References

1. P.N. Keating, Mol.Cryst.Liquid Cryst. 8, 315 (1969).

2. H. de Vries, Acta Cryst. 4, 219 (1951).

3. P. Kassubek and G. Meier, Mol. Cryst. Liquid Cryst. 8, 305 (1969).

4. P.G. de Gennes, Solid State Commun. 10, 753 (1972); Mol.Cryst.Liquid Cryst. 21, 49 (1973).

5. R. Alben, Mol.Cryst.Liquid Cryst. 20, 231 (1973).

6. R.S. Pindak, C.C. Huang and J.T. Ho, Phys. Rev. Letters, 32, 43 (1974).

7. R.S. Pindak, C.C. Huang and J.T. Ho, Solid State Commun. 14, 821 (1974).

8. P. Pollmann and H. Stegemeyer, Chem.Phys.Letters 20, 87 (1973).

9. P. Pollmann and H. Stegemeyer, Berichte der Bunsen-Gesellschaft f. Physikalische Chemie, 78, 843 (1974).

10. P. Pollmann and G. Scherer, Mol. Cryst. Liquid Cryst. Letters 34, 189 (1977).

11. P. Pollmann and G. Scherer, Chem.Phys.Letters 47, 286 (1977).

12. P.H. Keyes, H.T. Weston and W.B. Daniels, Phys. Rev. Letters, 31, 628 (1973).

See also R. Shashidhar and S. Chandrasekhar, J. Physique, 36, C1-49 (1975).

13. R. Shashidhar, Mol. Cryst. Liquid Cryst. 43, 71 (1977).